

**ROTARY KILN PRODUCT QUALITY  
FORECASTING BASED ON FLAME IMAGING****Carl Duchesne <sup>\*\*</sup>,<sup>1</sup> André Desbiens <sup>\*\*\*</sup>,<sup>1</sup>  
Gerard Szatvanyi <sup>\*\*</sup>***LOOP (Laboratoire d'observation et d'optimisation des  
procédés - Process observation and optimization  
laboratory)**\*\* Department of Chemical Engineering**\*\*\* Department of Electrical and Computer Engineering**Université Laval, Pavillon Adrien-Pouliot**Québec City (Québec), Canada G1K 7P4**Email: Carl.Duchesne@gch.ulaval.ca*

Abstract: For most applications, the rotary kiln product quality control problem is to apply a certain temperature profile to the solids within the kiln through direct contact with a hot flue gas produced by combustion. Since it is very difficult to measure the solids temperature profile in the kiln, due to the harsh environment and the rotating motion of the shell, quality control is often achieved in practice by controlling the solids discharge temperature close to some target value. The rationale behind that is twofold: 1) the solids discharge temperature is often highly correlated to *Copyright © 2006 IFAC*

Keywords: Image analysis, Multivariate quality control, Industrial control, Prediction, Forecasts

**1. INTRODUCTION**

Rotary kilns are frequently used in the chemical and mineral processing industries since they can accommodate the production of various kinds of products over a wide range of operating conditions. These very versatile process equipments are used for the calcination of lime and coke, the pyrolysis of various kinds of wastes, and for ore roasting and sintering. They are also used to dry a wide variety of products, such as fish and Soya meal, minerals, sawdust, and grain, bark, coal, fertilizer, and other aggregates. Rotary kilns are, however, very complex systems involving simultaneous solid-gas heat and mass transfer coupled to chemical reactions and solids transportation

problems. Fundamental modelling of these systems to improve understanding and operational practices is still a very active research area (Finnie *et al.*, 2005).

For most applications, the rotary kiln product quality control problem is to apply a certain temperature profile to the solids within the kiln through direct contact with a hot flue gas produced by combustion. Since it is very difficult to measure the solids temperature profile in the kiln, due to the harsh environment and the rotating motion of the shell, quality control is often achieved in practice by controlling the solids discharge temperature close to some target value. The rationale behind that is twofold: 1) the solids discharge temperature is often highly correlated to product quality measured in the laboratory,

<sup>1</sup> Supported by NSERC (Canada).

and 2) this temperature is easier to measure with good accuracy using IR pyrometers, which also provides more frequent measurements than laboratory quality analyses (in the order of seconds instead of a few times per day). The typical quality control strategy is to maintain the solids discharge temperature above a lower limit, below which product quality starts degrading (production loss), and below an upper limit, above which the kiln automatically shuts down for safety reasons. In the latter case, several minutes are required to restart the kiln and also involve production losses. Achieving a solids discharge temperature within these limits is, however, no longer sufficient due to constantly increasing fuel costs and the pressure to reduce CO<sub>2</sub> emissions (e.g. Kyoto agreement) and other combustion pollutants such as CO, NO<sub>x</sub> and SO<sub>2</sub>. The solution to simultaneously reduce gaseous emissions and fuel consumption while maintaining the desired product quality is to reduce temperature variations as much as possible to bring its target value closer to the lower temperature limit (i.e. reduce overheating).

Reducing discharge temperature variability is difficult since this amount in reducing variations in the heat released by the combustion process. In most rotary kiln applications, turbulent non-premixed combustion is used, which means that combustion and mixing of the fuel and the oxidizer (e.g. air) occur simultaneously, at the burner tip. This type of combustion process is more chaotic and difficult to control than when the fuel and air are premixed and then burned (Yu and MacGregor, 2004). Moreover, the secondary air flow rate is not always measured (but changed using fans), and several rotary kilns are operated using multiple sources of fuel having different heats of combustion.

Implementing feedback controllers on such a rotary kiln to control the discharge temperature using, for example, total fuel flow rate as the manipulated variable is the first step in reducing variability. However, these kilns have long dead-times and slow dynamics and are affected by several sources of unmeasured disturbances, several of them introduced by the combustion process itself. To further reduce discharge temperature (quality) variability ones need to predict the impact of these unmeasured disturbance and to forecast them in the future. This is very difficult to do with the actual instrumentation due to the absence of internal state measurements. The main contribution of this work is to provide one such internal state sensor to forecast product quality using images of the combustion flame taken within the kiln. This new sensor could be used in conjunction with any process control strategy and would fit particularly well into a Model Predictive Control

(MPC) framework. It can also be of great help to operators when the kilns are manually controlled, as is often the case in industry.

Flame imaging has already been investigated in the past, but most of these contributions were performed on laboratory scale combustion systems and premixed flames, and their approach was to compute geometrical and luminous properties of the flame extracted from gray scale images and use them to either classify the flame into arbitrarily defined states (Bertuccio *et al.*, 2000; Victor *et al.*, 1991) or to predict various quantities such as flicker rate (Huang *et al.*, 1999), unburnt carbon, CO<sub>2</sub> and NO<sub>x</sub> emissions (Shimoda *et al.*, 1990; Lu *et al.*, 1999; Yan *et al.*, 2002) or fuel and air flow rates (Tao and Burkhardt, 1995). Only a few past investigations were extracting the flame features from RGB color images (Wang *et al.*, 2002; Keyvan, 2003) and were taking advantage of the three wavelengths to estimate the flame temperature distribution using the bicolor method. Finally, a few research works analyzed the flames using spectrometers (Keyvan, 2003) from which it is possible to extract more precise chemical information about the radicals present in the flame. An additional limitation of these approaches consists of extracting the flame visual features directly from the image space. Since the flame is turbulent, it bounces around continuously and hence, extracting the flame visual characteristics requires finding the location of the flame boundaries for each image. This step increases computation time and might cause difficulties for on-line monitoring of highly turbulent flames. This problem has recently been addressed by Yu and MacGregor (Yu and MacGregor, 2004) who applied the Multivariate Image Analysis (MIA) technique to RGB images of non-premixed turbulent flames from an industrial boiler. This method will be used in this work to build a dynamic model between the flame image and solids discharge temperature.

The rest of this paper is organized as follows: the industrial rotary kiln system is presented in Section 2, as well as the data and flame images collected from it. In Section 3, Multivariate Image Analysis and Regression (MIA and MIR) methods to extract the features of flame images and to regress them against discharge temperature (product quality) are presented. Three approaches for forecasting the product quality are described and compared in Section 4: forecasts based on flame images, on an autoregressive model and finally by combining both preceding techniques with a Kalman filter. Finally, some conclusions are drawn in Section 5.

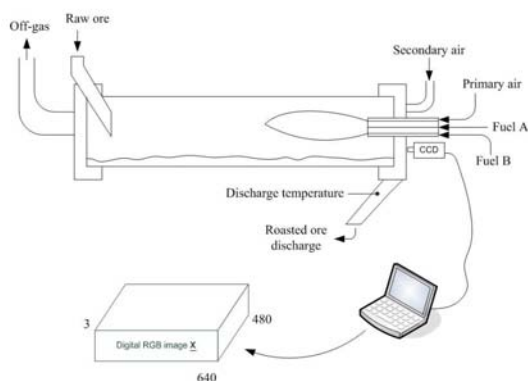


Fig. 1. Rotary kiln and imaging system setup

## 2. INDUSTRIAL PROCESS AND COLLECTED DATA AND IMAGES

The rotary kiln studied in this work is shown in Figure 1, along with the flame monitoring system. A total of four of these kilns are currently operated by QIT-Fer et Titane inc. (Sorel-Tracy, Quebec, Canada), each of them are about 220 ft long and have a diameter of about 12 ft. The kiln is used to apply a heat treatment to raw ore by a direct contact with a hot gas flowing in countercurrent with the solids. The mean residence time of the solids within the kiln is currently about 80 minutes as determined by the rotational speed and the inclination of the kiln, as well as the solids throughput. A number of thermocouples are inserted through the kiln shell at different locations along the kiln length. However, these are considered unreliable by operators and engineers. They are located in an extremely harsh environment and would require frequent maintenance to ensure reliable readings, which can be performed only during shutdowns since they rotate with the shell. Only the roasted ore (final product) discharge temperature obtained using an IR pyrometer is considered to be a reliable solids temperature measurement. The solids discharge temperature is strongly related to roasted ore quality and is currently used by operators for quality control since laboratory quality measurements are only available every few hours and are obtained from a composite sample of all the kilns. It is the variations in the discharge temperature that will be modeled using flame imaging.

The combustion takes place at the solids discharge end of the kiln. Two types of fuel as well as primary air are fed to the burner tip from three concentric pipes without premixing. The flow rates of primary air and the two fuel types are measured on-line. Fuel A is produced in another part of the plant and both its flow rate and heat of combustion vary. The flow rate of fuel B (supplied to the plant) is adjusted to maintain heat released by the combustion, based on a relationship involving

Periods	Date	Number of frames
1	May 2004	2526
2	June-July 2004	6730
3	August 2004	1839
4	November 2004	23134
5	February 2005	46229
Total:		80458

Table 1. Summary of collected images

the ratio of standard heat of combustion of each fuel. Finally, secondary air is also blown in the kiln to support complete combustion and to maintain a certain amount of excess oxygen in off-gas for safety considerations. Secondary air flow rate is not currently measured, but changed using fans.

The color CCD video camera (JVC TK-C1380) is installed in a small opening just behind the burner. An air-cooling device is used to protect the CCD from damage caused by high temperatures. The output signal of the camera is sent to a portable computer located in the control room, where the frames are digitized using a frame grabber card. Each of the resulting digital image forms a three way array or a "cube" of data consisting of 640 x 480 pixels (spatial dimensions) and, for each of these pixels, the light intensity in the red (R), the green (G), and the blue (B) colors are stored in the third dimension of the cube (i.e. the spectral dimension is 3). The RGB light intensities vary between 0 and 255 with a resolution of 24 bytes.

To develop prediction models for solids discharge temperature (quality), a total of 80458 such images were collected over time at a rate of 1 frame every 10 seconds. Images were intentionally gathered at different periods during year 2004-2005 to capture any seasonal variations and to test the robustness of the prediction models. Table 1 summarizes the five image collection periods.

On-line kiln operation data was also collected and synchronized with the flame images. About 50 measurements currently are available around the kilns. However, the most relevant measurements for this work were solids throughput and discharge temperature, as well as the following combustion related variables: fuel (A and B) and primary air flow rates, fuel ratio and total fuel flow rate, and the shutter position of the secondary air blower.

## 3. FEATURE EXTRACTION AND REGRESSION BASED ON MIA AND MIR

### 3.1 Extraction of Flame Image Features using MIA

Prior to developing models between flame images and solids discharge temperature, ones needs to extract the features of flame images in order to formulate the regression problem. It has been shown

by Yu and MacGregor (Yu and MacGregor, 2004) that flame color features can be efficiently extracted using a MIA technique, since it classifies the image pixels according to their spectral characteristics (e.g. combinations of RGB intensities) without considering their spatial position. This means that flames having a similar coloration (i.e. similar heat release) will be projected in a similar region of the MIA low dimensional feature space even if they are located differently in the image. This is a very useful characteristic since the objective of this work is to develop a model between heat released by the flames (i.e. flame color) and product quality rather than tracking the position of highly turbulent flames that bounce around constantly. MIA therefore allows extracting flame information without first locating the flame within the image. This is a major advantage compared to conventional flame image analysis techniques used in previous research working directly in the image space, hence requiring additional computing time.

The MIA technique will be briefly discussed here, but for more details the reader is referred to Geladi and Grahn (Geladi and Grahn, 1996) and to a few of papers (Yu *et al.*, 2003) using this technique for various quality control applications. MIA essentially consists in performing a Multi-Way Principal Component Analysis (MPCA) on a digital multivariate image. This involves two steps. First, the digital image  $\underline{\mathbf{X}}$  is unfolded from a three-way array to a two-way matrix  $\mathbf{X}$ :

$$\underline{\mathbf{X}}_{(N_{row}, N_{col}, N_{spect})} \xrightarrow{\text{unfold}} \mathbf{X}_{(N_{row} \times N_{col}, N_{spect})} \quad (1)$$

where  $N_{row}$  and  $N_{col}$  correspond to the spatial dimensions of the image (640 and 480 in this study), whereas the third dimension or spectral dimension is identified by  $N_{spect}$ . Since the images have three spectral channels (R, G, and B),  $N_{spect}$  equals 3. This unfolding operation collects the RGB intensities of each pixel row wise in matrix  $\mathbf{X}$ . Second, PCA is performed on the unfolded digital image  $\mathbf{X}$ :

$$\mathbf{X} = \sum_{a=1}^K \mathbf{t}_a \mathbf{p}_a^T + \mathbf{E} \quad (2)$$

where  $K$  is the number of principal components, the  $\mathbf{t}_a$  vectors are the score vectors, and the corresponding  $\mathbf{p}_a$  vectors are the loading vectors. For RGB images, the maximum number of components is 3. If  $K < 3$ , then  $\mathbf{E}$  contains the residuals of the PCA decomposition. A kernel algorithm is typically used to compute this decomposition since  $\mathbf{X}$  has a very large number of rows ( $N = 640 \times 480 = 307200$ ) and a small number of columns (3). In this algorithm, the loadings vectors ( $\mathbf{p}_a$ ) are obtained from a singular value decomposition (SVD) of the very low dimensional kernel matrix  $\mathbf{X}^T \mathbf{X}$  (only  $3 \times 3$  for an RGB image). The score

vectors are then computed using  $\mathbf{t}_a = \mathbf{X} \mathbf{p}_a$ . The MIA technique as described previously is used for the analysis of a single image. When MIA is to be used for the analysis of a set of  $J$  images, then the kernel matrix is calculated as  $\sum_{i=1}^J \mathbf{X}_i^T \mathbf{X}_i$  and then SVD is performed on that summation matrix to calculate the loading vectors.

As for the analysis of data matrices using PCA, the interpretation of image features is performed using score plots, and particularly  $t_1 - t_2$  score plots since in most MIA applications using RGB images, the first two principal components explain most of the variance (Yu and MacGregor, 2004). However, due to the very large number of score values typically encountered in image analysis (total number of pixels or 307200 for a  $640 \times 480$  image), the score plots are usually displayed as 2-D density histograms and shown as images themselves to enhance their visual appearance. To obtain such a score histogram, denoted as  $\mathbf{TT}$ , the  $t_1 - t_2$  score plots is first divided into a number of bins, usually  $256 \times 256$ , and the pixels falling into each bin are then counted and stored in matrix  $\mathbf{TT}$  at the corresponding bin location. After selecting a proper color map proportional to the pixel density in each bin, the 2-D score density histogram  $\mathbf{TT}$  ( $256 \times 256 \times 1$ ) can be displayed as an image. When a set of images are analyzed using MIA, a common scaling range is used for the scores prior to compute the density histograms. This scaling range corresponds to the minimum and maximum values of all  $t_1$  and  $t_2$  score vectors of the set of images.

An alternative way to interpret the image information is to refold the  $\mathbf{t}_a$  ( $N_{row} \times N_{col} \times 1$ ) score vectors in a three-way array  $\mathbf{T}_a$  ( $N_{row} \times N_{col} \times 1$ ) according to the same spatial coordinates as in the original image  $\underline{\mathbf{X}}$  (i.e. pixel locations), and then show each  $\mathbf{T}_a$  as a univariate image. This is useful to visually identify the information extracted from the original image by each principal component (Yu and MacGregor, 2004).

### 3.2 Multivariate Image Regressionsubsec:MIR)

The aim of this work is to build a dynamic model between the flame color features extracted from each image and the corresponding solids discharge temperature measurement (i.e. quality variable). This can be accomplished using Multivariate Image Regression (MIR), which refers to a family of techniques used for regressing quality or response variables on image features. Image regression problems can be formulated in several ways, depending on the image feature extraction method. In this study, solids discharge temperature is regressed on the  $t_1 - t_2$  score density histograms (i.e. distribution features) obtained from

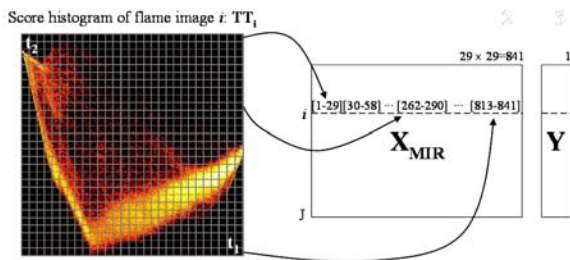


Fig. 2. Multivariate Image Regression (MIR) problem formulation

flame images using MIA (see previous section). However, prior to build regression models, one needs to solve the dimensionality issue arising from the fact that for each score histogram (i.e. a matrix of dimension  $N_{bt1} \times N_{bt2}$ ) correspond a single temperature measurement (i.e. a scalar). Dimensions  $N_{bt1}$  and  $N_{bt2}$  are the number of bins dividing the score plot along the  $t_1$  and  $t_2$  score axes respectively. This problem was addressed by storing the elements of each score histogram matrix (i.e. number of pixels falling into each bin) row wise in a new matrix  $\mathbf{X}_{MIR}$  as follows:

$$\begin{aligned} \mathbf{X}_{MIR}(i, 1 : N_{bt1} \times N_{bt2}) = & \\ [\mathbf{TT}_i(1, 1 : N_{bt1}) \quad \mathbf{TT}_i(2, 1 : N_{bt1}) \quad \dots & \\ \dots \quad \mathbf{TT}_i(N_{bt2}, 1 : N_{bt1})] & \quad (3) \\ i = 1, 2, \dots, J & \end{aligned}$$

This procedure is schematically shown in Figure 2 for the score histogram of flame image  $i$  ( $\mathbf{TT}_i$ ) with  $N_{bt1} = N_{bt2} = 29$  (i.e. score histogram divided using a grid of  $29 \times 29$ ). In this way, the  $t_1 - t_2$  score density histogram information obtained for image  $i$  is all contained in row  $i$  of  $\mathbf{X}_{MIR}$  whereas the corresponding quality measurement is stored in the  $i^{th}$  row of the quality matrix  $\mathbf{Y}$ . Any appropriate regression method can then be used to build a model between  $\mathbf{X}_{MIR}$  and  $\mathbf{Y}$ , such as Ordinary Least Squares (OLS), Partial Least Squares (PLS), etc. For this regression to be meaningful, however, one must absolutely make sure that a common scaling range has been applied to the  $t_1 - t_2$  score density histograms before storing their elements in  $\mathbf{X}_{MIR}$ , and that these elements are always stored in the same order to preserve information congruency.

Finally, dividing score plots using a grid of  $256 \times 256$  is appropriate for image interpretation and visualization using MIA as discussed in Section 3.1. For image regression purposes, however, such a resolution is often unnecessarily high, and would unduly increase computing time and memory requirements. Most previous work on MIR make use of a  $32 \times 32$  grid. After some testing, a grid of  $29 \times 29$  bins was selected for convenience, but no further improvements in the results were obtained by increasing the grid resolution.

Model	A	B	C	D
Forecast (min)	0	+5	+10	+15
$R_{X,cum}^2$ (%)	59.8	59.9	59.9	59.8
$R_{Y,cum}^2$ (%)	79.7	76.4	71.9	68.3
$Q_{X,cum}^2$ (%)	77.8	74.4	69.4	66.0
RMSEP	16.22	17.35	18.20	19.10
Model	E	F	G	H
Forecast (min)	+20	+40	+60	+80
$R_{X,cum}^2$ (%)	52.9	53.3	53.3	53.2
$R_{Y,cum}^2$ (%)	61.8	49.1	37.2	28.3
$Q_{X,cum}^2$ (%)	60.3	47.1	34.8	25.3
RMSEP	20.13	22.82	25.30	27.01

Table 2. Summary statistics for the various dynamic models between flame images and solids discharge temperature

#### 4. PREDICTION RESULTS

A subset of the data discussed in Section 2 was used to build dynamic models between the color features of flame images and solids discharge temperature. After removing outliers, only the data for which no operation disruption (kiln shutdown) occurred within an 80 minutes window from current time was kept for model development. From the 80458 original images, only 53300 satisfied the above criteria and were kept for model building and validation.

The summary statistics for each prediction model are presented in Table reftab:stats. It shows the number of PLS components (A) used for each MIR model determined by cross-validation, three cumulative multiple correlation coefficients ( $R_{X,cum}^2$ ,  $R_{Y,cum}^2$ , and  $Q_{X,cum}^2$ ), and the root mean square prediction errors (RMSEP). The  $R_{X,cum}^2$  statistics correspond to the percentage of the total variance in the image information (X) used to explain Y whereas  $R_{Y,cum}^2$  gives the percentage of the total variance of Y explained by the model. The cumulative  $Q_{X,cum}^2$  value is the percentage of the total variance of Y that can be predicted by the models using a leave-one-out cross validation procedure. Model A shows a very interesting result which is about 80% of the discharge temperature variations are explained by the flame color features, and hence are related to variations in the combustion process. The remaining 20% may be caused by feed disturbances (i.e. changes in moisture content and solids composition and feed rate) and measurement noise. This confirms that stabilizing the combustion process could significantly reduce temperature variations and therefore shows the importance of monitoring the flame and kiln walls. As the forecast horizon increases from 0 to 80 minutes in the future, the rate of increase in the RMSEP is lower than linear. Predicting discharge temperature  $t + 80$  minutes in the future using as the only the image color feature at time  $t$  as the only source of information still allow to explain as much as 30% of the variations.

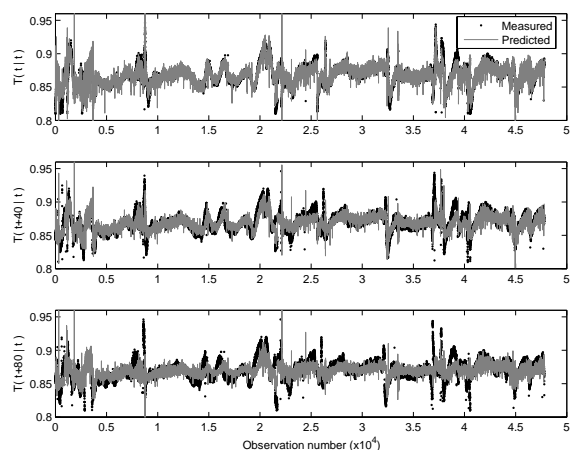


Fig. 3. Measured and predicted discharge temperature at time  $t$ ,  $t + 40$  and  $t + 80$  minutes in the future using the flame image collected at time  $t$  (model A, F, and H respectively)

Figure 3 shows the prediction performance of models A, F, and H on a validation data set, consisting of 48000 images not used for model building (only 5300 images were used for model development). A very good agreement between the time series, even for model H. ....

## 5. CONCLUSION

When ran simultaneously, models A-H will provide a temperature forecast from time  $t$  to time  $t + 80$  minutes, which will be very useful for kiln operators to take appropriate control decisions, when the kiln is manually operated. This set of temperature predictions could also be incorporated into various predictive control schemes when automatic kiln control is preferred. In future work, ways to improve discharge temperature forecasts by adding past images to that one collected at time  $t$  will be investigated. This is not trivial since each image contains large amounts of information. Combining the current prediction models with past temperature measurements into an ARMA time series models framework is considered. How to used the image information for combustion control and discharge temperature (quality) control will also be investigated.

## REFERENCES

Bertucco, L., A. Fichera, G. Nunnari and A. Pagano (2000). A cellular neural networks approach to flame image analysis for combustion monitoring. In: *Proceedings of the 6th IEEE International Workshop on Cellular Neural Networks and Their Applications*. pp. 455–459.

Finnie, G.J., N.P. Kruyt, M. Ye, C. Zeilstra and J.A.M. Kuipers (2005). Longitudinal and

transverse mixing in rotary kilns: A discrete element method approach. *Chemical Engineering Science* **60**, 4083–4091.

Geladi, P. and H. Grahn (1996). *Multivariate Image Analysis*. Wiley. Chichester, UK.

Huang, Y., Y. Yan, G. Lu and A. Reed (1999). On-line flicker measurement of gaseous flames by image processing and spectral analysis. *Meas. Sci. Technol.* **10**, 726–733.

Keyvan, S. (2003). Diagnostics and control of natural gas fired furnaces via flame image analysis. In: *Sensors and Automation FY03 Annual Review Meeting*. Office of Industrial Technologies, Energy Efficiency and Renewable Energy. US Department of Energy.

Lu, G., Y. Yan, Y. Huang and A. Reed (1999). An intelligent vision system for monitoring and control of combustion flames. *Measurement and Control* **32**, 164–168.

Shimoda, M., A. Sugano, T. Kimura, Y. Watanabe and K. Ishiyama (1990). Prediction methods of unburnt carbon for coal fired utility boiler using image processing technique of combustion flame. *IEEE Transactions on Energy Conversion* **5**, 640–645.

Tao, W. and H. Burkhardt (1995). Vision-guided flame control using fuzzy logic and neural networks. *Particle and Particle System Characterisation* **12**, 87–94.

Victor, J., J. Costeira, J. Tomé and J. Sentieiro (1991). A computer vision system for the characterization and classification of flames in glass furnaces. In: *Conference Record of the IEEE Industry Applications Society Annual Meeting*. pp. 1109–1117.

Wang, F., X.J. Wang, Z.Y. Ma, J.H. Yan, Y. Chi, C.Y. Wei, M.J. Ni and K.F. Cen (2002). The research on the estimation for the nox emissive concentration of the pulverized coal by the flame image processing technique. *Fuel* **81**, 2113–2120.

Yan, Y., G. Lu and M. Colechin (2002). Monitoring and characterisation of pulverized coal flames using digital imaging techniques. *Fuel* **81**, 647–656.

Yu, H. and J.F. MacGregor (2004). Monitoring flames in an industrial boiler using multivariate image analysis. *AIChE J.* **50**, 1474–1483.

Yu, H., J.F. MacGregor, G. Haarsma and W. Bourg (2003). Digital imaging for on-line monitoring and control of industrial snack food processes. *Ind. Eng. Chem. Res.* **42**, 3036–3044.